

# ROBUST IRIS FEATURE EXTRACTION AND MATCHING

*S. Rakshit and D. M. Monro*

Department of Electronic and Electrical Engineering, University of Bath, BA2 7AY, UK  
<http://dmsun4.bath.ac.uk> {s.rakshit, d.m.monro}@bath.ac.uk

## ABSTRACT

An iris coding method based on zero crossings of Discrete Cosine Transform (DCT) coefficients between rectangular patches from normalized iris images is shown to provide excellent matching performance at low complexity. The method is applied to two sets of normalized iris images; 2156 images of 308 eyes from the CASIA database and 2955 images of 150 eyes from the Bath database. A product-of-sum approach to Hamming distance calculation is taken and 100% Correct Recognition Rate (CRR) achieved for identification. For verification, a variable threshold is applied to the distance metric and the False Acceptance and False Rejection Rates (FAR, FRR) recorded. The method achieves perfect Receiver Operating Characteristics (ROC), i.e. no false accepts or rejects are registered. A new metric for evaluating practical system performance is proposed and the theoretical equal error rate (EER) estimated from the Hamming Distance distributions is found to be as low as  $2.59 \times 10^{-4}$ .

## 1. INTRODUCTION

In this work we report a significant improvement in the feature extraction and matching performance of human iris recognition systems, which are an increasingly important form of biometric identity authentication [1]. We use zero crossings of the Discrete Cosine Transform (DCT) as a means of feature extraction for iris matching.

The human iris is a thin circular diaphragm lying between the cornea and the lens. Apart from general textural appearance and color, the detailed fine structure of an iris develops by random processes during embryonic development and is unique to every eye [2]. Being an externally visible internal organ and essentially stable over a person's lifetime, the iris lends itself to non-invasive and accurate identification. Pioneering work in iris coding was done by Daugman using Gabor wavelets [3]. Other researchers including Wildes et al. [4], Ma et al. [5], and Monro et al. [6] have contributed alternative iris coding techniques.

The paper is subdivided as follows. Section 2 motivates the use of the DCT for feature extraction. The proposed iris coding method is presented and its parameters tuned in Section 3. Results are tabulated with statistical analysis in Section 4, and conclusions drawn in Section 5.

## 2. THE DISCRETE COSINE TRANSFORM

The proposed approach falls into the category of objective, non-semantic methods of pattern analysis. The use of the Karhunen-Loeve Transform (KLT) for object recognition [7] and in particular, face recognition [8] are examples of this approach. The advantage of such methods is derived from the automatic generation of suitable feature vectors by a transform such as the KLT. The KLT decomposes an image into principal components, ordered on the basis of spatial correlation and is statistically

optimal in the sense that it minimizes the mean square error between a truncated representation and the actual data [7]. This provides a variance distribution that decreases rapidly with the order of the transform, i.e. it has optimal energy compaction properties.

The DCT is a real valued transform whose variance distribution resembles that of the KLT with much lower computational complexity [9]. Due to its good energy compaction properties the DCT is widely used for data compression. In addition the feature extraction capabilities of the DCT coupled with well known fast computation techniques [10] have made it a candidate for pattern recognition problems such as the one addressed here. In particular, the DCT has been shown to produce good results on face recognition [11], where it has been used as a less computationally intensive replacement for the Karhunen-Loeve transform (KLT).

Although no transform can be said to be optimal for recognition, these properties motivated us to investigate the DCT for effective non-semantic feature extraction from human iris images. There are several variants of the DCT but the one most commonly used operates on a real sequence  $x_n$  of length  $N$  to produce coefficients  $C_k$ , following Ahmed et al. [12]:

$$C_k = \frac{2}{N} w(k) \sum_{n=0}^{N-1} x_n \cos\left(\frac{2n+1}{2N} \pi k\right), \quad 0 \leq k \leq N-1$$

and,

$$x_n = \sum_{k=0}^{N-1} w(k) C_k \cos\left(\frac{2n+1}{2N} \pi k\right), \quad 0 \leq n \leq N-1$$

where  $w(k) = \frac{1}{\sqrt{2}}$  for  $k = 0$  and  $w(k) = 1$  for  $1 \leq k \leq N-1$

## 3. PROPOSED IRIS CODING METHOD

The primary objective behind any good iris coding method is to obtain good inter-class separation in minimum time. Here, we discuss the new method in detail with its various parameters optimized for best system performance.

### 3.1 Localization and normalization

Iris coding is normally carried out on an image that consists wholly or predominantly of iris texture. It is usual to identify the pupil and iris outlines, and then map the annulus of the iris onto a rectangular image with suitable grayscale adjustments to preserve iris detail while removing variations in background illumination as illustrated in Fig. 1. Additionally, the iris may be partly obscured by eyelids and eyelashes, and these regions need to be masked prior to feature extraction. Detailed description of the various image processing tasks involved in obtaining such a 'normalized' image is beyond the scope of this paper.

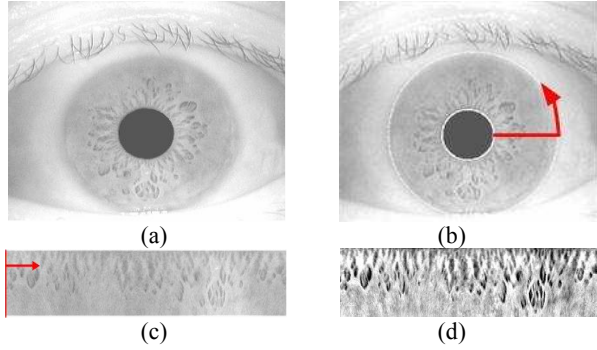


Fig 1. Iris Image Pre-Processing. (a) Original Image; (b) Localized Image; (c) Unwrapped Image; and (d) Enhanced Image.

In this work, we start from two data sets of normalized iris images, one of 2156 images of 308 classes (eyes) which is widely available from the CASIA [13], and the other of 2155 images of 150 classes from our own measurements [14]. The normalized images are 512 pixels in the horizontal (radial) direction and 80 pixels in the vertical (radial) direction. For coding we use the 48 vertical (radial) pixels nearest the pupil to mitigate the effect of eyelashes and eyelids.

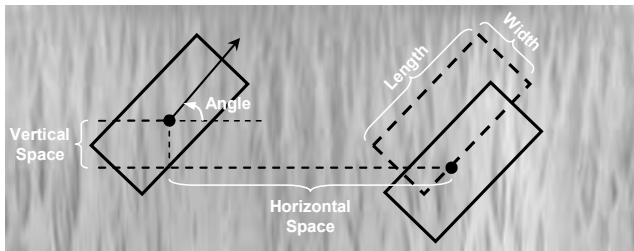


Fig. 2. Overlapping angular patches with their various parameters.

### 3.2 Feature Extraction

In our coding scheme, feature vectors are derived from the zero crossings of the differences between DCT coefficients calculated in rectangular image patches, as illustrated by Fig. 2. Averaging across the width of these patches with appropriate windowing smoothes the data and mitigates the effects of noise and other image artifacts. A 1D DCT then codes each patch along its length at low computational cost. Values of the various parameters were tuned over the CASIA and Bath databases to obtain the best predicted Equal Error Rate (EER).

Fig. 3. shows four such EER optimizations; for patch length, width, angle and horizontal spacing. Horizontally aligned overlapping diagonal patches produced the best EER in combination with the other parameters. The optimum parameters were incorporated into the coding method. To form image patches, diagonal patches were selected in 11 overlapping horizontal bands. Each patch is 12 pixels wide (overlapping by 6) and 8 pixels long (overlapping by 4). Over the 12 pixel width, a weighted average under a  $\frac{1}{4}$  Hanning window is formed, to reduce the degrading effects of noise. Along the length (45 degrees from the iris radial), the 8 averaged values form a 1D patch vector, which is then windowed using a similar Hanning window prior to application of the DCT. The differences between the DCT coefficients of adjacent patch vectors are then calculated and their zero crossings give us an 8 bit ‘codelet’.

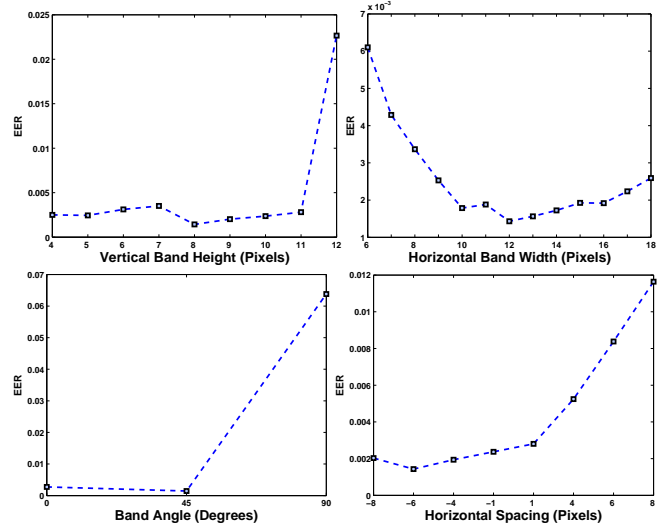


Fig. 3. EER optimizations plots for patch length, patch width, patch angle and horizontal spacing.

The feature vector length is reduced by extracting the most discriminating codelet bits. By coding both sets of data for every combination of bits, the best separation between the matching and non-matching Hamming distances were obtained using bits 1-3 of the binarized DCT codelet. With 781 such subfeatures, the final feature length was 2343 bits.

### 3.3 Matching

For comparing two iris codes the distance between two feature vectors was calculated using the product-of-sum (POS) of individual subfeature Hamming distances (HD) as defined below:

$$HD = \left( \prod_{i=1}^M \frac{\sum_{j=1}^N (SubFeature 1_{ij} \oplus SubFeature 2_{ij})}{N} \right)^{1/M}$$

Here, the iris code is considered to be a rectangular block of size  $M \times N$ ,  $M$  being the number of bits per subfeature (3), and  $N$  the total number of subfeatures in a feature vector (781). Corresponding subfeature bits are XORed and the resultant  $N$ -length vector is summed and normalized by dividing by  $N$  to give the normalized HD lying in the range of 0 to 1. For a perfect match, every bit from Feature 1 matches the corresponding bit of Feature 2, and the HD is 0. For a totally reversed code where every bit from the first Feature is reversed in the second the HD is 1. Since a total bit reversal is highly unlikely, it is expected that a random pattern difference should produce a HD of around 0.5.

While our previous HD calculation [6] was based on a weighted sum of EXOR-ed bits, the new POS method provides for better separation by skewing the matching distribution towards 0 and the non-matching one towards 0.5.

Rotation invariance is achieved by storing six additional iris codes for three rotations on either side by horizontal (iris circumferential) shifts of 4, 8 and 12 pixels each way in the normalized images. During verification, the test iris code is compared against all seven stored ones and the minimum distance chosen for each of the three separately enrolled images. These three minima are then averaged to give the final matching HD.

## 4. RESULTS

For both datasets, three arbitrary images were chosen from each class to be enrolled in the database, leaving the rest for testing. Both Identification and Verification tasks were evaluated. For Identification, a test image was coded and compared against the whole database of stored features. The comparison giving the lowest average HD across the three enrolled images for all classes was chosen as the matching iris. 100% Correct Recognition Rates were obtained on both the CASIA and Bath datasets.

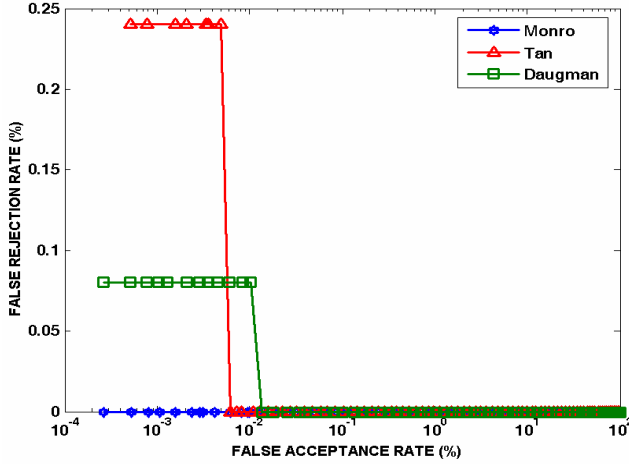


Fig. 4. ROC Curves for Daugman, Tan and proposed algorithms.

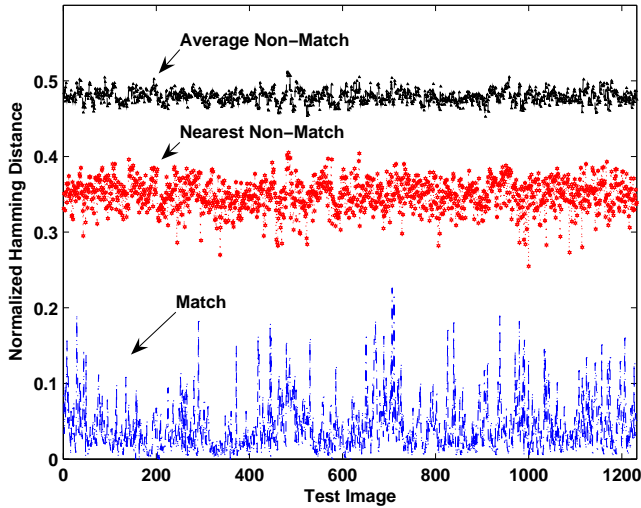


Fig. 5. Line plots of average non-match, nearest non-match and matching iris images for the CASIA Database

For Verification, ROC curves were generated by varying a match-cutoff threshold from 0 to 1 and plotting the FRR as a function of the FAR. Fig. 4. illustrates the ROC curves on the CASIA database for the three algorithms compared. All comparisons were carried out at feature extraction level on the same set of pre-normalized images in order to achieve a fair comparison. On the CASIA data set a single false rejection causes a step jump of 0.08% in the FRR while 3 false rejects cause a rise of 0.24%. These small numbers of failures are not themselves sufficient for drawing statistically significant comparisons but are shown in keeping with the general

practice of showing ROC curves for comparing algorithms. Similar curves were obtained on the Bath database.

In our previous work on FFT based coding [6], the only False Rejection was found at a FAR of  $2 \times 10^{-3}$ %. In this work the ROC is perfect, i.e. there are no false rejects because matching and non-matching distributions in the available data are completely separated, so the DCT based method is an improvement on the FFT method. For a better evaluation of the effectiveness of the DCT method, we turn to statistical modeling of the matching and non-matching Hamming distances.

The proposed algorithm performance is better illustrated by plotting the matching, nearest non-matching and average non-matching normalized Hamming distances for all test images as shown in Fig. 5 for the CASIA dataset. An important figure of merit for a biometric system is the Equal Error Rate (EER), which is equal to the FAR and FRR when they are equal. In case of no failures the actual EER cannot be estimated and in the absence of thousands or millions of cases for testing, the EER must be predicted by statistical modeling. In Fig. 6, we show the two probability distributions of matching and nearest non-matching Hamming distances for the three algorithms studied.

With each distribution normalized for unit area, the area under the matching distribution above a chosen HD threshold ( $\tau$ ) is the FRR, while that under the non-matching distribution below the same threshold is the FAR. Thus, the EER is the area such that the integral from  $-\infty$  to  $\tau$  of the non-matching distribution is equal to the integral from  $\tau$  to  $\infty$  for the matching distribution. When the non-matching distribution is compared against the nearest non-match, the estimated EER is a more stringent metric than it would be if the average non-match is used instead of the latter. We call this the worst case EER. Additionally, comparing the lowest HD from the non-match set with the matching one is a more realistic comparison since real systems fail when the HD of the second best match falls below the correct match HD. A distinct space between these two plots imply that there will be no false accepts or rejects for a significant range of match-thresholds as neither plot will cross over to the other side for any test image. From Fig. 6. it is evident that the matching and nearest non-matching data are not as well separated by the Daugman and Tan algorithms in the implementations we used as they are by the proposed DCT code.

Experimental observations showed that the matching Hamming distances were best modelled by Gamma distributions in a least square error sense, while Weibull distributions were appropriate for the nearest non-matches. On the Bath dataset the estimated EER for the proposed method was found to be  $2.59 \times 10^{-4}$ . The estimated EERs for the Tan and Daugman algorithms were  $8.9 \times 10^{-3}$  and  $4.9 \times 10^{-3}$  respectively. It must be noted here that these estimates are based on the more stringent and practically relevant basis of comparing the matches with the nearest non-match.

Speed comparisons of MATLAB implementations were carried out for the three algorithms studied. The total time taken by feature extraction and matching of the proposed method is 61 ms as against 193 ms taken by the Tan method and 453 ms taken by Daugman's algorithm. The main speed gain occurred in the feature extraction stage where the simplicity of application of the 1D DCT helped speed up the entire process compared to the more computationally intensive procedures adopted by other methods. It should be noted that all figures are based on MATLAB implementations and are to be interpreted on a relative scale only. Implementations in real systems are likely to be many times faster.

## 5. CONCLUSIONS

We have presented an improved approach to human iris recognition based on the 1D Discrete Cosine Transform (DCT). The work was motivated by the known properties of the DCT, and good performance was achieved where the predicted EER is the lowest amongst the coding algorithms compared on the CASIA and Bath datasets. Additionally the low complexity of the proposed method makes it superior to the other methods evaluated in terms of both speed and accuracy. We have demonstrated the use of novel patch encoding methods in capturing iris texture information, proposed the worst case (nearest non-match) EER as a new practical metric for evaluating system performance and investigated better classifier designs for inter-class separability. Statistical analysis has also been carried out to find good models for the matching and non-matching probability distributions so that Equal Error Rates can be predicted even where no failures occur.

Because performance depends on the effectiveness of iris image localization and normalization, all comparisons were made on the same sets of normalized images. There remain many challenges in preprocessing of human iris images which as they are met will further enhance the performance of this and other iris matching techniques.

## 6. ACKNOWLEDGMENTS

This work was sponsored by Smart Sensors Limited, Portishead, Bristol, BS20 7BA, United Kingdom. We thank Professor Tienui Tan, Chinese Academy of Sciences Institute of Automation for the use of the CASIA iris image databases, and Dr Li Ma of CASIA for his implementations of the Tan and Daugman algorithms.

## 7. REFERENCES

- [1] A. K. Jain, A. Ross, and S. Prabhakar, "An Introduction to Biometric Recognition," *IEEE Trans. Circuits and Systems for Video Tech.*, vol. 14, pp. 4 - 20, 2004.
- [2] P. Kronfeld, *Gross anatomy and embryology of the eye*, in: H. Davson (Ed.), *The Eye*. London: Academic Press, 1962.
- [3] J. Daugman, "High confidence visual recognition of persons by a test of statistical independence," *IEEE Trans. PAMI*, vol. 15, pp. 1148 - 1161, 1993.
- [4] R. P. Wildes, "Iris recognition: an emerging biometric technology," *Proc. of the IEEE*, vol. 85, pp. 1348 - 1363, 1997.
- [5] L. Ma, T. Tan, Y. Wang, and D. Zhang, "Efficient iris recognition by characterizing key local variations," *IEEE Trans. on Image Processing*, vol. 13, pp. 739 - 750, 2004.
- [6] D. M. Monro and D. Zhang, "An effective human iris code with low complexity," presented at IEEE ICIP, 2005.
- [7] M. Uenohara and T. Kanade, "Use of Fourier and Karhunen-Loeve decomposition for fast pattern matching with a large set of templates," *IEEE Trans. PAMI*, vol. 19, pp. 891-898, 1997.
- [8] M. Turk and A. Pentland, "Eigenspaces for Recognition," *Journal of Cognitive Neuroscience*, vol. 3, 1991.
- [9] K. R. Rao and P. Yip, *Discrete Cosine Transform: Algorithms, Advantages, Applications*. New York, NY: Academic, 1990.
- [10] M. Vetterli, "Fast 2-D discrete cosine transform," *Proc. IEEE ICASSP*, pp. 1538-1541, 1985.
- [11] Z. M. Hafed and M. D. Levine, "Face Recognition Using the Discrete Cosine Transform," *International Journal of Computer Vision*, vol. 43, pp. 167-188, 2001.
- [12] N. Ahmed, T. Natarajan, and K. Rao, "Discrete cosine transform," *IEEE Trans. on Computers*, vol. 23, pp. 90-93, 1974.
- [13] "CASIA Iris Image Database, <http://www.sinobiometrics.com>."
- [14] "University of Bath Iris Image Database, <http://www.bath.ac.uk/elec-eng/pages/sipg/irisweb/>."

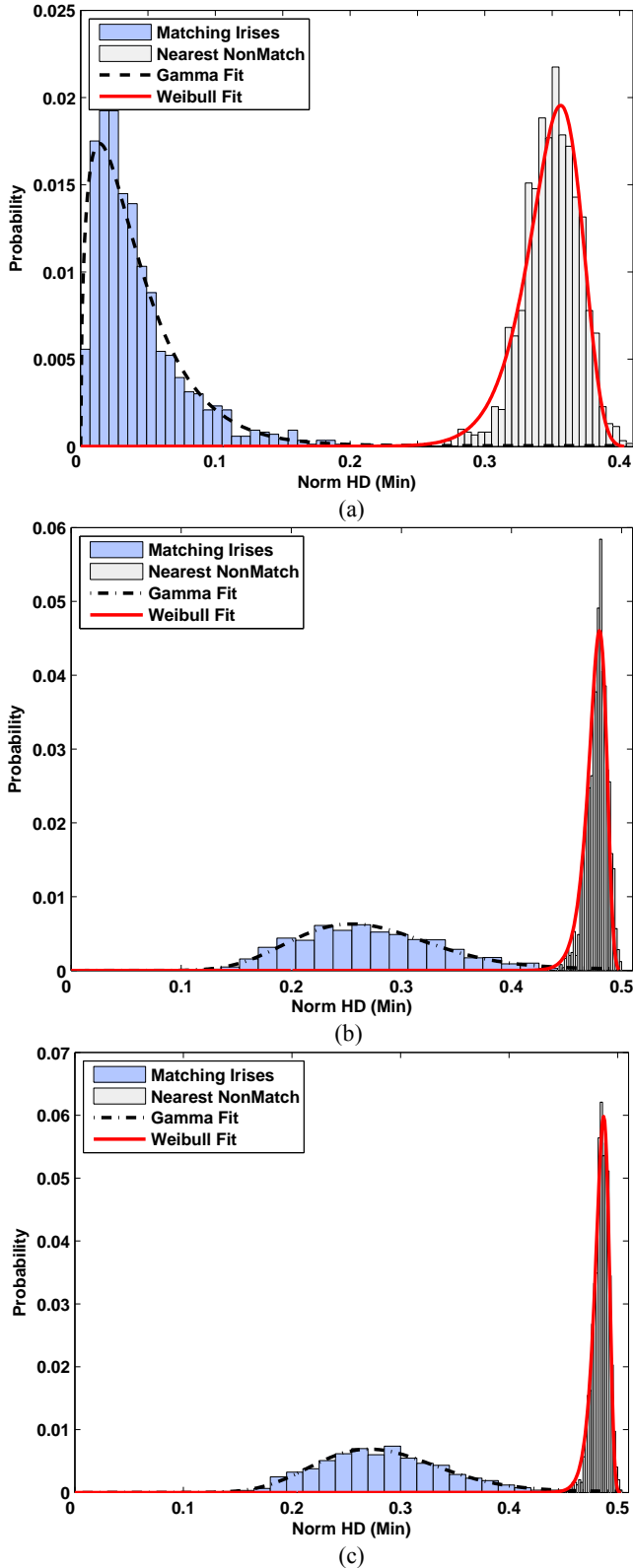


Fig. 6. Probability distributions for matching and nearest nonmatching hamming distances for (a) proposed; (b) Tan and (c) Daugman algorithms on the CASIA dataset.